Fluorescent Probes

DOI: 10.1002/anie.201007386

An Effective Minor Groove Binder as a Red Fluorescent Marker for Live-Cell DNA Imaging and Quantification**

Xiaojun Peng, Tong Wu, Jiangli Fan, Jingyun Wang, Si Zhang, Fengling Song, and Shiguo Sun*

Since the understanding of DNA organization and structure in vivo is so important, fluorescent staining techniques using organic DNA-binding molecules are required for biological research and medical diagnosis, including cellular imaging and DNA quantification.[1–5] However, membrane-permeable DNA-specific stains are uncommon. The minor groove binders 4′,6-diamidino-2-phenylindole (DAPI) and Hoechst 33258 are presently used for DNA-specific staining,[6] but they require ultraviolet excitation, which can lead to cellular damage due to lengthy irradiation.[7] SYTO stains do provide cell-permeable dyes excitable by visible and near-infrared radiation. Unfortunately they are not specific nuclear stains,[6] and moreover are of undisclosed chemical structures. Although the cell-permeant anthraquinone dye DRAQ5 shows red fluorescence emission and DNA-specific labeling, it is a DNA intercalator, which seriously interferes with the structure and function of nuclear DNA, in contrast to the minor groove binders such as SYTO17.[8]

Therefore, a pressing need exists to develop fluorescent dyes satisfying the multiple criteria of long-wavelength excitation/emission, high DNA selectivity, and live-cell permeability. Recently, a terbium complex $[Tb{\cdot}L^2]^{+}$[2] was described which stained the nuclear DNA in mitotic cells using very low dye concentrations ($<1\ \mu M$). Unfortunately, intense irradiation of 350 nm is needed as excitation light. BENA435,[3] with an *N*,*N*-dimethylpropane-1,3-diamine group, was reported to stain the nucleus in live cells, but still with excitation/emission located at the cyan region ($\lambda_{ex(DNA)} = 435$ nm; $\lambda_{em(DNA)} = 485$ nm). Chang et al.[4] have discovered an excellent DNA-selective probe, C61, with relatively long emission wavelength ($\lambda_{em(DNA)} = 540$ nm) for live-cell nuclear imaging and DNA quantification. C61 shows a 19.9-fold fluorescence increase when bound to double-stranded (ds) DNA ($\Phi_F{}^{DNA} = 0.0675$). Another promising finding has been reported by Thomas et al.,[5] namely that a dinuclear ruthenium(II) polypyridyl complex ($\lambda_{em(DNA)} = 680$ nm) can be used as a nuclear DNA stain for both luminescence and transmission electron microscopy. Despite the high hydrophilicity and charge of the molecule, it was still taken up by live cells, but only if a relatively high concentration of more than 200 μM was used. In fluorescence microscopic imaging studies, it is desirable for DNA staining to involve large fluorescence enhancements, and for nuclei to stain rapidly even when low concentrations of dye are used, as this minimizes dye toxicity to live cells.

Herein, we report a novel red fluorescent dye DEAB-TO-3 (Scheme 1, DEAB = (diethylamino)butyl)), a TO-3 analogue with long-wavelength excitation and emission

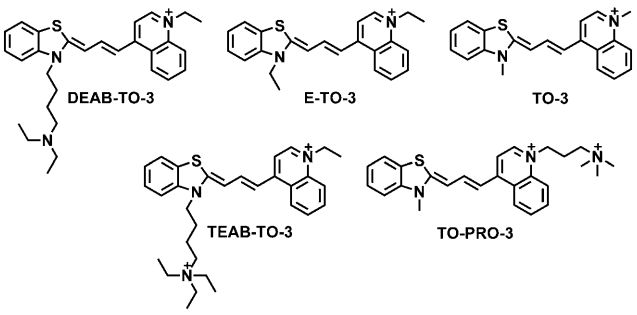

Scheme 1. Chemical structures of DEAB-TO-3, TEAB-TO-3, TO-PRO-3, E-TO-3, and TO-3.

($\lambda_{abs(DNA)} = 626$ nm and $\lambda_{em(DNA)} = 649$ nm), to meet the above demands. Notably, besides avoiding cellular autofluorescence interference, another advantage of a red fluorescent dye is its applicability with a red semiconductor laser (energy line 633 nm) as light source. This laser is much smaller in size and more stable than an argon-ion laser (energy lines 488, 514 nm). DEAB-TO-3 shows a very low intrinsic fluorescence in aqueous solution ($\Phi_F{}^{free} = 0.0037$), which is of prime importance for a fluorescent probe for DNA detection. Upon binding to calf thymus (CT) DNA, the quantum yield of DEAB-TO-3 increased 97.3-fold ($\Phi_F{}^{DNA} = 0.36$), much larger than the 13.5-fold increase of the commercially available dye ethidium bromide (EB) under the same conditions (Figure 1).

Furthermore, DEAB-TO-3 fluoresces four times more strongly in the presence of AT sequences (80.3-fold increase of fluorescence) than GC sequences (18.9-fold), although it has very similar affinity for poly(dA-dT)$_2$ and poly(dG-dC)$_2$ (see Figure S1 in the Supporting Information). Previous work has shown that intramolecular twisting is an efficient quenching pathway of unsymmetrical cyanine dyes in unconstrained environments, and the huge increase of fluorescence quantum

[*] Prof. X. Peng, T. Wu, J. Fan, S. Zhang, F. Song, S. Sun
State Key Laboratory of Fine Chemicals
Dalian University of Technology
2 Linggong Road, 116024 Dalian (China)
E-mail: pengxj@dlut.edu.cn
Prof. J. Wang
School of Life Science & Biotechnology
Dalian University of Technology (China)

[**] We thank the NSF of China (Nos. 20725621, 20876024, 21076032, 21072024, and 21006009), the National Basic Research Program of China (2009CB724706), and the Cultivation Fund of the Key Scientific and Technical Innovation Project (707016) for support of this work. We also thank Dr. Richard W. Horobin for advice on the estimation of log*P* values.

Supporting information for this article is available on the WWW under http://dx.doi.org/10.1002/anie.201007386.

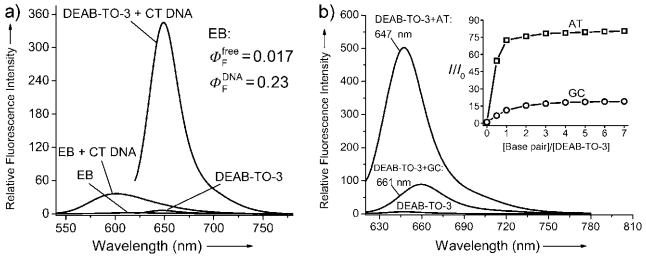

Figure 1. a) Fluorescence emission spectra of DEAB-TO-3 (1 μM) and EB (1 μM) in the absence and presence of CT DNA in buffer at 20 °C. b) Fluorescence emission spectra and enhancement of fluorescence intensities during the titration of a solution of DEAB-TO-3 (1 μM) with poly(dA-dT)$_2$ and poly(dG-dC)$_2$ at 20 °C. Inset: The [base pair]/[DEAB-TO-3] molar ratios are from 0.5 to 7. Quantum yield was measured in Tris–HCl buffer (pH 7.4). Rhodamine B in methanol was used as a standard.

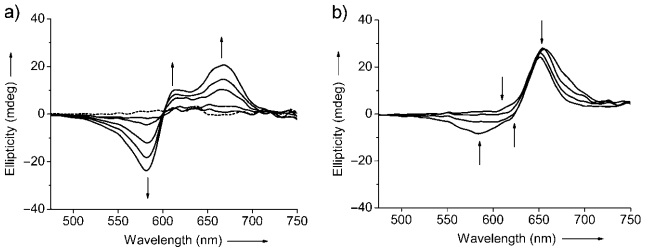

Figure 3. CD spectra during the titration of a 14 μM solution of DEAB-TO-3 with CT DNA at 20 °C in buffer. The [base pair]/[DEAB-TO-3] molar ratios are 0.33, 0.63, 1.25, 1.67, and 2.5 in (a) and 15, 20, 30, and 45 in (b). The black dashed line refers to DEAB-TO-3 without CT DNA. The arrows indicate how the CD bands respond to the increases in the CT DNA concentration.

yield upon binding to DNA originates from the loss of mobility in the constrictive DNA environment.[9] So the light-up difference between binding to AT and GC segments can mainly be ascribed to the different deactivation pathways of the excited state (probably resulting from different binding modes with AT and GC segments) of DEAB-TO-3. Specifically, fluorescence can be quenched in GC-rich regions by photoinduced electron transfer (PET) with the guanine bases,[3,10] which also accounts for the much lower fluorescence increase of DEAB-TO-3 in the presence of GC sequences.

The shapes of both the electronic bands and induced circular dichroism (ICD) bands seen during the titration of DEAB-TO-3 with CT DNA indicate that DEAB-TO-3 binds with a great contribution of minor groove binding to native DNA. Based on the work reported by Hannah and Armitage,[11] the blue-shifted band as complex I ($\lambda_{max} = 586$ nm) shown in Figure 2 can be explained by the face-to-face stacking of two molecules of DEAB-TO-3, forming an "H" dimer. When two dimers of DEAB-TO-3 are assembled adjacent to one another in the minor groove, a secondary coupling arises because of the end–end interaction between dimers.[11] This is normally manifested as a split blue-shifted band displayed as the negative circular dichroism (CD) band at 580 nm and positive CD band at 616 nm in the CD spectrum (Figure 3a). For complex II ($\lambda_{max} = 626$ nm), a corresponding transition is seen as the rather small negative

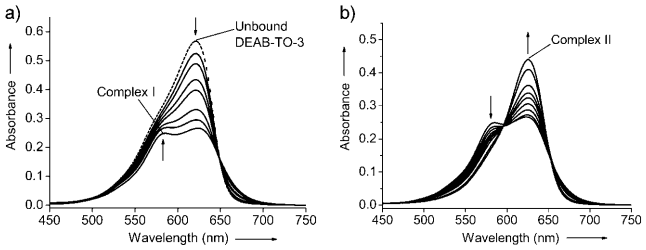

Figure 2. Absorption spectra during the titration of a 5 μM solution of DEAB-TO-3 with CT DNA at 20 °C in buffer. The [base pair]/[DEAB-TO-3] molar ratios are 0.33, 0.63, 1.25, 1.67, 2.5, 3.3, and 5 in (a) and 6.5, 8, 10, 12.5, 15, 20, 30, 45, and 60 in (b). The black dashed line refers to DEAB-TO-3 without CT DNA. The arrows indicate how the absorption bands respond to the increases in the CT DNA concentration.

CD band at 618 nm and positive CD band at 654 nm, then finally the single positive CD band at 652 nm (Figure 3b). It is noteworthy that, besides the hypochromicity and red-shift phenomena of the absorption band, the obvious increases of viscosity and T_m of CT DNA (see Figures S3 and S4 in the Supporting Information) caused by the addition of DEAB-TO-3 well support our suggestion that DEAB-TO-3 displays multiple and cooperative associations with the genomic DNA.

Unlike DEAB-TO-3, the methyl-substituted TO-3 (Scheme 1) shows a half-intercalation binding (no minor groove binding was seen) with dsDNA at a high [base pair]/[TO-3] molar ratio (see Figures S5 and S6 in the Supporting Information). Similar results are also obtained from the ethyl-substituted E-TO-3 (Scheme 1). So for groove binding to occur with this type of conjugated structure, inhibition of intercalation by steric hindrance resulting from bulky substituents (such as the bulky (diethylamino)butyl group in DEAB-TO-3) on the DNA probe is necessary.

Early studies had reported that although staining of cell nuclei was observed for TO-PRO-3, TO-PRO-1, YO-PRO-3, and propidium iodide (PI), only TO-PRO-3 showed specific staining of this structure.[12] Moreover, all of these highly hydrophilic dyes are impermeable to live cells. TEAB-TO-3 (Scheme 1, $\log P_{cation} = -5.2$) with a cationic side chain showed a very similar staining result to that of TO-PRO-3 ($\log P_{cation} = -5.0$). On the other hand, E-TO-3 (Scheme 1, $\log P_{cation} = -0.3$) was monocationic and only slightly hydrophilic. Whilst the protonated dicationic species of DEAB-TO-3 is more strongly hydrophilic ($\log P_{dication} = -4.1$), the nonprotonated monocationic species, which will also be present under physiological conditions, is less hydrophilic ($\log P_{monocation} = -2.0$) and so DEAB-TO-3 will be membrane permeable. Of these two dyes only DEAB-TO-3 gave strong staining of nuclear chromatin, with faint cytoplasmic staining in two cell lines (Figure 4). E-TO-3, on the other hand, was less selective, giving stronger staining of cytoplasm. This is perhaps a consequence of the much more bulky nature of the substituent of DEAB-TO-3, as discussed above.

Both dual staining and ribonuclease (RNase) digestion experiments (see Figures S8 and S9 in the Supporting Information) indicated that the cytoplasmic staining seen with E-TO-3 resulted from dye binding to ribosomal RNA. It may be noted in passing that DEAB-TO-3 (both the

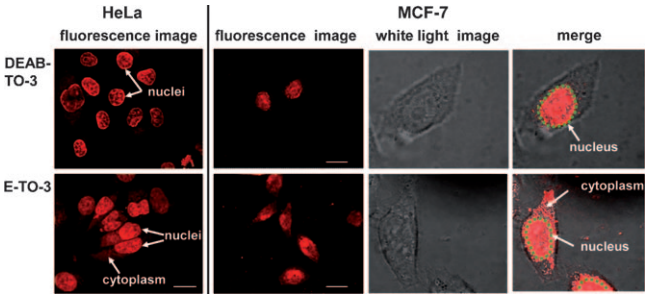

Figure 4. Live-cell staining with DEAB-TO-3 and E-TO-3. Both dyes were tested at a 5 μM concentration for HeLa cells and 2 μM for MCF-7 cells. A 1000× magnification was utilized in the imaging. Scale bars: 20 μm. DEAB-TO-3 and E-TO-3 (red: Cy5 channel) are shown. The white light and the merge images were obtained by enlarging one cell shown in the fluorescence image of MCF-7 cells.

monocationic and dicationic species) fits all the criteria for a selective nuclear probe in terms of size of the planar aromatic system, base strength, and log*P* as specified in the quantitative structure–activity relationship (QSAR) model of Horobin's group.[13] Generally, we were able to get an excellent fluorescence signal of the stained cells at 2 μM for DEAB-TO-3. Moreover, it is noteworthy that DEAB-TO-3 works in both live and fixed cells, which allows various experimental options for cellular imaging.

For many DNA dyes, avoiding the nonspecific binding to cellular RNA, protein, and other biomacromolecules is a critical problem in DNA labeling and measurement.[6,12] Therefore, a set of solution assays was carried out to investigate the selectivity of DEAB-TO-3 to DNA in vitro. As shown in Figure 5a, the fluorescence of DEAB-TO-3

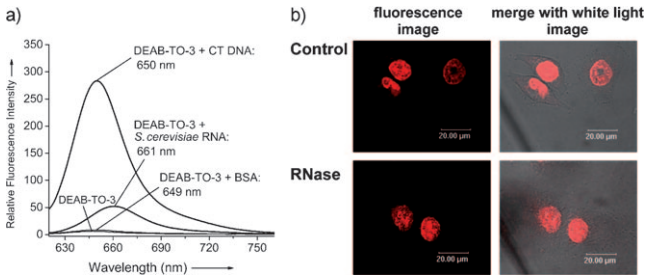

Figure 5. a) Fluorescence emission spectra of DEAB-TO-3 in the absence and presence of CT DNA, *S. cerevisiae* RNA, and BSA in buffer at 20 °C. b) RNase digestion experiment of DEAB-TO-3 (2 μM). Live MCF-7 cell images of DEAB-TO-3 (2 μM) are shown as a control; equal exposure was used for dye imaging. A 1000× magnification was utilized in the imaging. Scale bars: 20 μm. DEAB-TO-3 (red: Cy5 channel) is shown.

increases 45.5-fold upon binding to the CT DNA, which is about six times more than that when bound to the same amount of *Saccharomyces cerevisiae* RNA (eightfold increase of fluorescence). Bovine serum albumin (BSA) was tested as a representative protein to investigate the possibility of protein binding in the cytoplasm and membrane of subcellular structures.[14] As shown in Figure 5a, DEAB-TO-3 showed almost no change of fluorescence response to BSA. Moreover, an RNase digestion experiment was performed to further confirm the DNA selectivity of DEAB-TO-3 in live cells. As shown in Figure 5b, the nuclear fluorescence intensity was hardly altered by RNAse digestion. Although not a 100% DNA-selective probe, DEAB-TO-3 has proved superior to commercially available DNA probes such as cell-impermeant EB, PI, thiazole orange homodimer (TOTO), and the cell-permeant SYTO dyes, which always need treatment with nucleases to distinguish between RNA and DNA in cells.[6,12]

Since cell cycle analysis by flow cytometry is a significant application of DNA-specific probes, DEAB-TO-3 was tested for quantitation of DNA without RNase digestion. We prepared two distinct cell populations: 1) normal PC12 cells and 2) PC12 cells induced by glutamate. Since glutamate-induced apoptosis[15] can lead to the breakdown of the nucleus and result in decreased cellular DNA content, apoptotic peak sub-G_1 can be observed before the G_0 or G_1 peak. The results in Figure 6a and b clearly show that for DEAB-TO-3, little

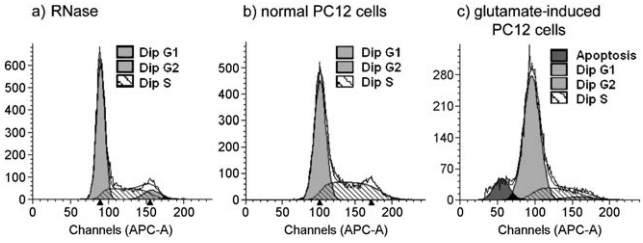

Figure 6. Cell cycle and apoptosis analysis. Normal PC12 cells (a, b) and glutamate-induced PC12 cells (c) were used in this experiment. The final concentration of DEAB-TO-3 was 1.12 μg mL^{-1} (2 μM). Values at vertical axes: number of cells.

difference (G_2/G_1, and peak shape) is observed between digestion with and without RNase for cell cycle analysis of normal PC12 cells. Even for the glutamate-induced apoptotic cells, the results shown in Figure 6c are acceptable (narrow peak), despite the difficulties arising from nuclear degradation. By contrast, PI was not capable of giving precise analysis unless the cells were digested with RNase (see Figure S10 in the Supporting Information). Note also that the final concentration of DEAB-TO-3 is 2 μM (1.12 μg mL^{-1}), which indicates a much higher sensitivity of DEAB-TO-3 than PI (120 μM; 50 μg mL^{-1}) and DRAQ5[16] (10 μM) in flow cytometry.

In summary, we have developed a TO-3 analogue DEAB-TO-3 ($\log P_{\text{monocation}} = -2.0$) with a (diethylamino)butyl substituent group playing a significant role in the whole structure. DEAB-TO-3 shows great fluorescence enhancement (97.3-fold) when bound to native DNA and a distinct selectivity for dsDNA over total RNA (six times). DEAB-TO-3, as a red fluorescent live-cell-permeant DNA minor groove binder, is a promising candidate for highly sensitive DNA detection in vitro and nucleus-specific imaging and DNA quantification in vivo.

Received: November 24, 2010
Published online: April 6, 2011

Keywords: cell cycle · DNA · fluorescent probes · imaging agents · nucleus staining

[1] L. J. Kricka, P. Fortina, *Clin. Chem.* **2009**, *55*, 670 – 683.

[2] G.-L. Law, C. Man, D. Parker, J. W. Walton, *Chem. Commun.* **2010**, *46*, 2391 – 2393.

[3] A. Erve, Y. Saoudi, S. Thirot, C. Guetta-Landras, J.-C. Florent, C.-H. Nguyen, D. S. Grierson, A. V. Popov, *Nucleic Acids Res.* **2006**, *34*, e43.

[4] S. Feng, Y. K. Kim, S. Yang, Y. T. Chang, *Chem. Commun.* **2010**, *46*, 436 – 438.

[5] M. R. Gill, J. Garcia-Lara, S. J. Foster, C. Smythe, G. Battaglia, J. A. Thomas, *Nat. Chem.* **2009**, *1*, 662 – 667.

[6] R. P. Haugland, *The Handbook: A Guide to Fluorescent Probes and Labeling Technologies*, **2005**, chap. 8.1. For more detailed information see the website: www.invitrogen.com/site/us/en/home/References/Molecular-Probes-The-Handbook.html.

[7] a) S. K. Davis, C. J. Bardeen, *Photochem. Photobiol.* **2003**, *77*, 675 – 679; b) G. P. Pfeifer, Y.-H. You, A. Besaratinia, *Mutat. Res.* **2005**, *571*, 19 – 31.

[8] a) P. J. Smith, N. Blunt, M. Wiltshire, T. Hoy, P. Teesdale-Spittle, M. R. Craven, J. V. Watson, W. B. Amos, R. J. Errington, L. H. Patterson, *Cytometry* **2000**, *40*, 280 – 291; b) K. Wojcik, J. W. Dobrucki, *Cytometry Part A* **2008**, *73*, 555 – 562.

[9] a) A. Fürstenberg, M. D. Julliard, T. G. Deligeorgiev, N. I. Gadjev, A. A. Vasilev, E. Vauthey, *J. Am. Chem. Soc.* **2006**, *128*, 7661 – 7669; b) G. L. Silva, V. Ediz, D. Yaron, B. A. Armitage, *J. Am. Chem. Soc.* **2007**, *129*, 5710 – 5718.

[10] S. O. Kelley, J. K. Barton, *Science* **1999**, *283*, 375 – 381.

[11] K. C. Hannah, B. A. Armitage, *Acc. Chem. Res.* **2004**, *37*, 845 – 853.

[12] a) K. Bink, A. Walch, A. Feuchtinger, H. Eisenmann, P. Hutzler, H. Höfler, M. Werner, *Histochem. Cell Biol.* **2001**, *115*, 293 – 299; b) R. M. Martin, H. Leonhardt, M. C. Cardoso, *Cytometry Part A* **2005**, *67*, 45 – 52.

[13] R. W. Horobin, J. C. Stockert, F. Rashid-Doubell, *Histochem. Cell Biol.* **2006**, *126*, 165 – 175.

[14] a) P. J. Smith, L. H. Patterson, US 6468753B1, **2002**; b) P. Panda, Z. G. Li, M. Szczepanik, W. F. Patton, US 20090226954A1, **2009**.

[15] X. Chena, J. Liua, X. S. Gua, F. Ding, *Brain Res.* **2008**, *1238*, 189 – 198.

[16] P. J. Smith, N. Blunt, M. Wiltshire, T. Hoy, P. Teesdale-Spittle, M. R. Craven, J. V. Watson, W. B. Amos, R. J. Errington, L. H. Patterson, *Cytometry* **2000**, *40*, 280 – 291.

